The propagation of spark-produced N waves through turbulence

Bart Lipkens

Applied Research Laboratories
Mechanical Engineering Dept.
The University of Texas at Austin

Work supported by NASA Langley

Presentation at NASA HSR Sonic Boom Workshop
NASA Ames Research Center
May 12-14, 1993

A model experiment was designed and built to simulate the propagation of sonic booms through atmospheric turbulence. The setup of the model experiment is described briefly. Measurements of the N waves after they propagated across the turbulent velocity field reveal the same waveform distortion and change in rise time as for sonic booms.

The data from the model experiment is used to test sonic boom models. Some models yield predictions for the waveform distortion, while others give estimates of the rise time of the sonic booms.

A new theoretical model for the propagation of plane N waves through a turbulent medium is described.

Introduction.

- model experiment: - successful in simulating the propagation of sonic booms through atmospheric turbulence
  - setup and results

- model experiment data is used to test sonic boom models
  - waveform distortion models
  - rise time prediction models

- new theoretical model for the propagation of plane N waves through a turbulent medium

In the model experiment the N waves are generated by a spark source. The spark-produced N wave is a spherically spreading wave, but it is also possible to create a locally plane N wave by inserting a paraboloidal reflector. The mirror is positioned so that the spark gap is at the focus of the paraboloidal reflector.

A plane jet generates the turbulent velocity field. A centrifugal fan blows air into a plenum chamber. The jet is formed when the air exits the chamber through the nozzle. The jet nozzle velocity is controlled by a Variac variable voltage controller and by adjusting the width of the nozzle. The plane jet characteristics are measured by hot-wire anemometry.

The N waves are measured by a wide band condensor microphone. Rise times as small as 0.45 μs can be measured.

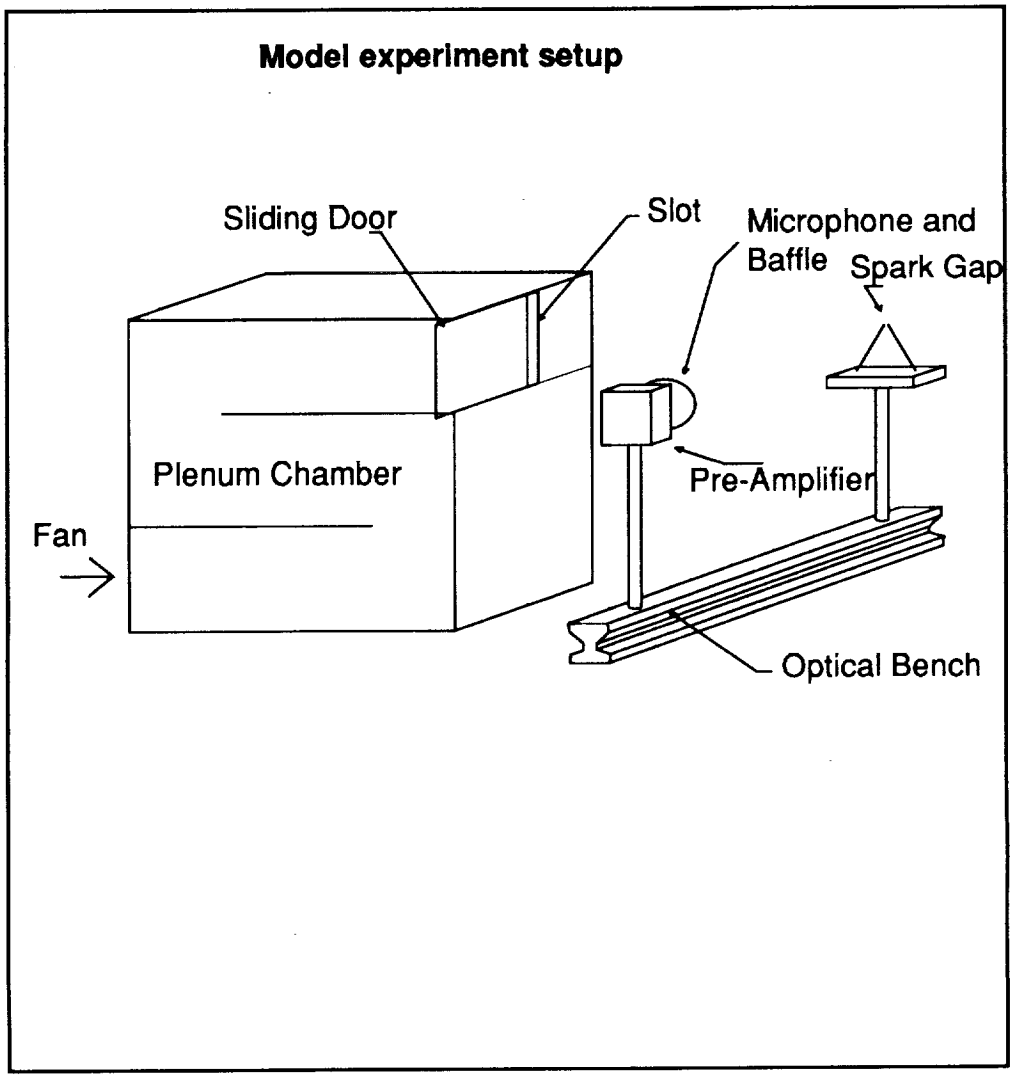

Examples of waveform distortion are shown. The upper left signature is that of a reference plane N wave recorded in the absence of turbulence. All other signatures represent waveforms measured after the plane N waves propagated through the turbulent velocity field. The distortion of the waveforms is similar as observed for sonic boom signatures. The distortion of the wavefront is most pronounced near the front and tail shocks. The fact that the distortion of the tail shock has the same pattern as that of the front shock is an indication that the turbulence is frozen during passage of the N wave. Variations in waveform from peaked to rounded and U-shaped are apparent. Double-peaked and multiple-peaked waveforms and messy wave shapes are also represented.

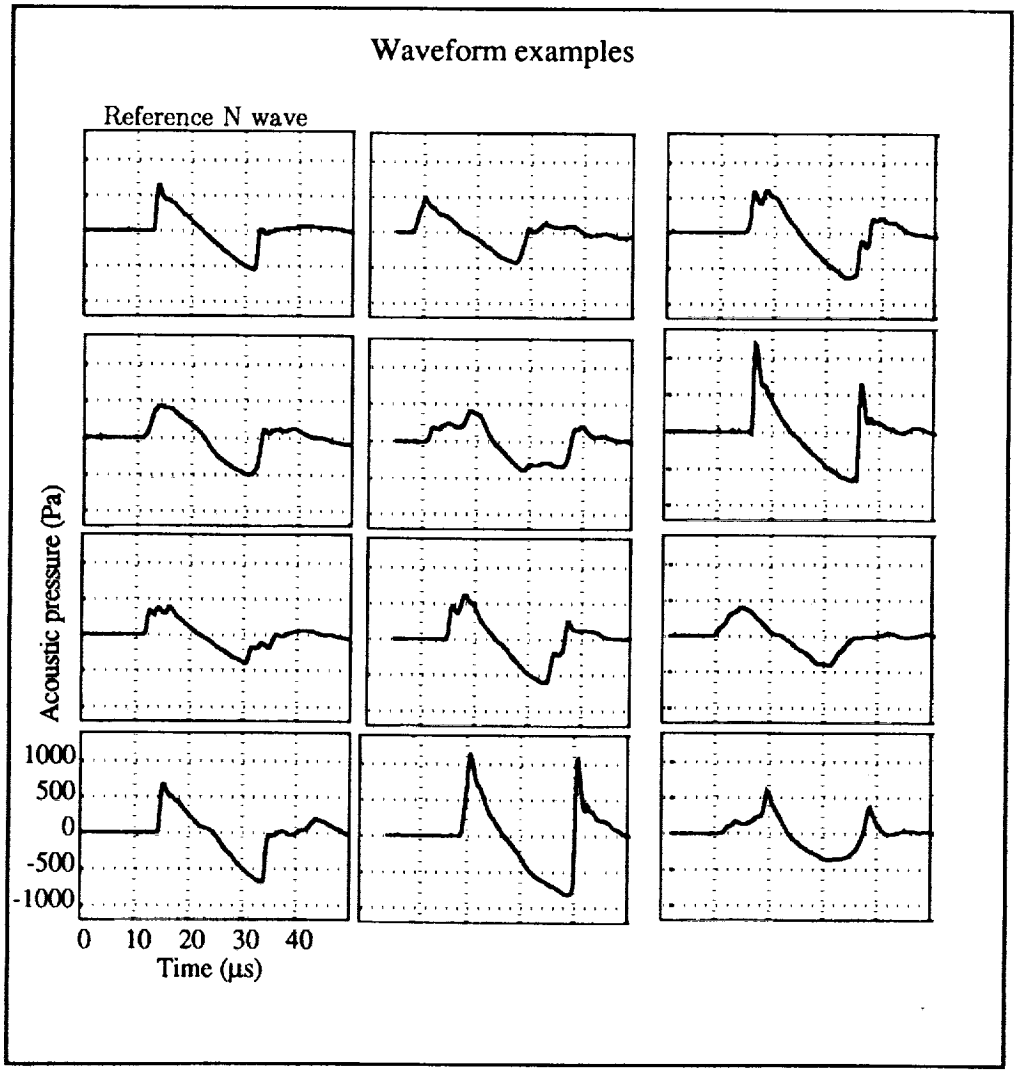

The first sonic boom model we review is Crow's waveform distortion model (Ref. 1). Crow's model is based on first order scattering theory. He modeled the sonic boom as a step shock of strength Δp. The mean-squared pressure perturbation equals $\langle p_S^2 \rangle = \Delta p^2 \, (t_c/t)^{7/6}$, where t_c is a critical time that is a function of the turbulence characteristics. The graph presents an example of the variance of an N wave for a value of $t_c = 2$ ms. A finite, very large value is obtained for the mean-squared pressure perturbation near the shock. Since the theory is a first-order scattering theory, both the incident and the scattered wave propagate at the ambient speed of sound c_0. However, from geometric acoustics we know that some ray paths might exist along which the actual propagation speed is faster than the ambient speed of sound. If we want to compare Crow's prediction with experimental data, then we have to shift the time origin of each sample waveform so that it begins at the time of shock arrival.

Testing of previous models

1. Crow's distortion model

- step shock : $\left\langle \psi^2(t) \right\rangle = (t_c/t)^{7/6} \qquad \psi(t) = p^S/\Delta p,$

$$t_c = \frac{1}{c_0} (\sec\theta)^{11/7} \left[\int_0^{h_f} 1.33 \, c_0^{-2} h^{5/6} \epsilon_u^{2/3} dh \right]^{6/7}$$

- Result of rms scattered pressure ($t_C = 2$ ms)

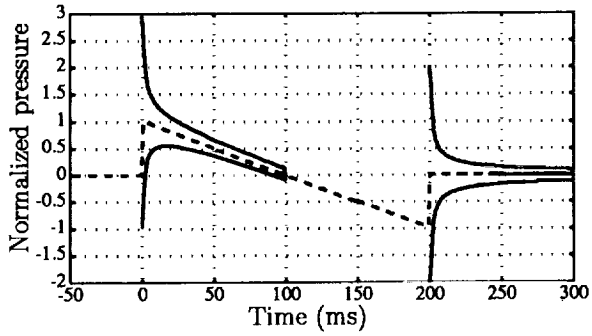

- Problems: $< \psi^2(0) > \approx 10^8$
  - incident wave of form f(x + c_0 t)
  - shock arrival time?
  - comparison with experiment?

Plotkin (Ref. 2) showed that an incident wave of arbitrary structure can be represented as a sum of infinitesimal step shocks. When the incident wave is modeled as a ramp shock instead of a step shock, an upper bound for the maximum pressure perturbation can be found, which is given by $\langle p_S^2 \rangle^{1/2} = \frac{12}{5} \Delta p \left(\frac{t_c}{t_0}\right)^{7/12}$, where t_0 is the rise time of the ramp shock.

Lipkens (Ref. 3) extended this model for an N wave. The rms pressure perturbation is presented in the first graph for an N wave with a rise time of 1 μs and a critical time of 0.33 μs. In order to calculate the rms pressure perturbation for the measured waveforms of the model experiment, we shifted the time origin of each waveform so that the times corresponding to 50 % of peak pressure all coincide.

A comparison between the measured distortion and Crow's prediction is presented in the lower graph. The measured distortion has the same general behavior as Crow's prediction, but the maximum pressure perturbation according to Crow's prediction is larger than the measured one by a factor of more than ten.

- Plotkin (1971): extension of Crow's model for a ramp shock
  - incident wave of arbitrary structure: sum of infinitesimal steps
  - upper bound for rms pressure perturbation

$$\left\langle (p_S)^2 \right\rangle_{\max}^{1/2} = \frac{12}{5} A \left(\frac{t_c}{t_0}\right)^{7/12}$$

- extension to N wave

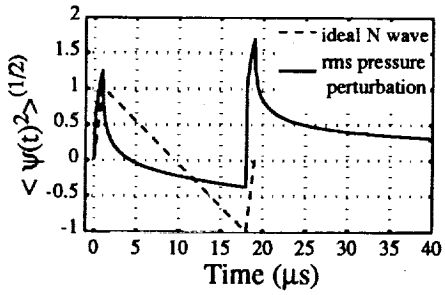

- measurements: shift each waveform --> 50 % peak pressure times coincide

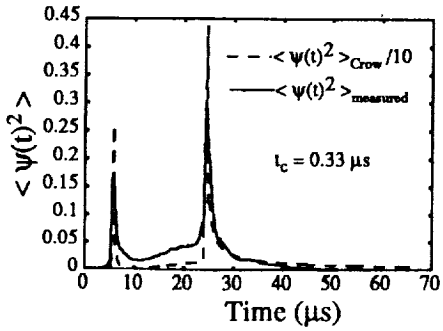

It is now widely accepted that molecular relaxation, especially that of nitrogen, is responsible for the large rise time of sonic booms. Controversy still exists whether turbulence has a pronounced effect on rise time. When a theory for the propagation of shock waves and transients through a turbulent medium is developed, it is important to incorporate the effect of shock arrival time correctly. The rise time of the stochastic mean of a set of waveforms represents an insignificant upper bound to the average of the rise times of each individual waveform. The graph shows a simple example that demonstrates that the rise time of the stochastic mean waveform of five step shocks, each having a rise time of 1 μs, is more than tenfold the average of the rise time of the individual realizations.

Rise time prediction models

- Turbulence cause of large rise time? What mechanism?

- Question of shock arrival time

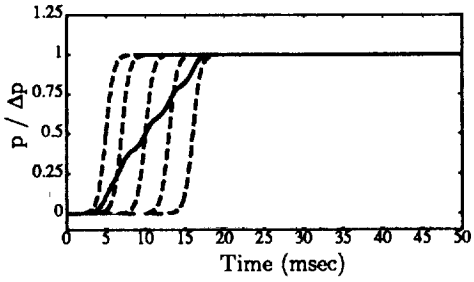

Pierce's model (Ref. 4) is based on the mechanism of wavefront folding at a caustic. If at a certain instant turbulence causes a ripple to develop on the shock front, a caustic is formed when the wavefront is propagated according to geometric acoustics. Inside the caustic three segments of the shock front arrive instead of one. Pierce argued that this process could occur many times if the turbulence intensity is large. A receiver then "sees" many segments of a multifolded wavefront at slighly different arrival times. The result is that instead of a sharp shock front a shock is received that consists of many smaller shocks at different arrival times. The overall result is a rounded shock front. The lower graph shows the mean waveform calculated according to Pierce's theory. Again, t_c is Crow's critical time.

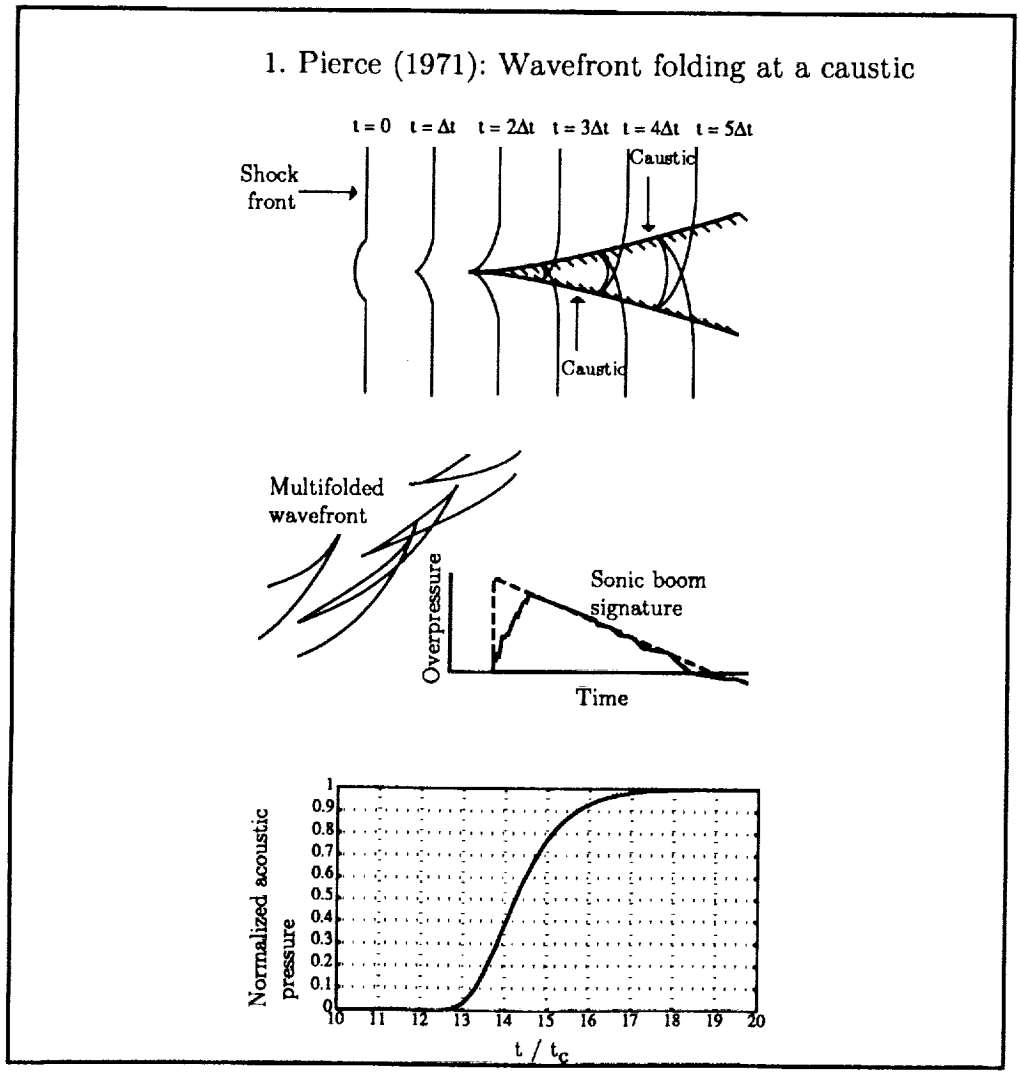

The mean waveform is expressed as a function of Crow's critical time t_c. The parameters E and b_1 are dependent on the structure of the atmospheric turbulence.

Again, the individual waveforms of the model experiment are shifted in order that times corresponding to 50 % of peak pressure coincide. The plot compares Pierce's prediction for the mean waveform and the computed mean of the shifted individual waveforms. A good agreement is reached.

In order to confirm this correlation, we performed an experiment at five different jet nozzle velocities. The comparison between Pierce's prediction and the measurements is fairly accurate. A maximum discrepancy of about 30 % is observed for a nozzle velocity of 31.3 m/s.

- mean waveform

$$\frac{\langle p(t) \rangle}{\Delta p_0} = \exp\left\{-E\hat{t}^{-1/6}e^{-b_1\hat{t}^{7/6}}\right\} \qquad \hat{t} = t/t_c$$

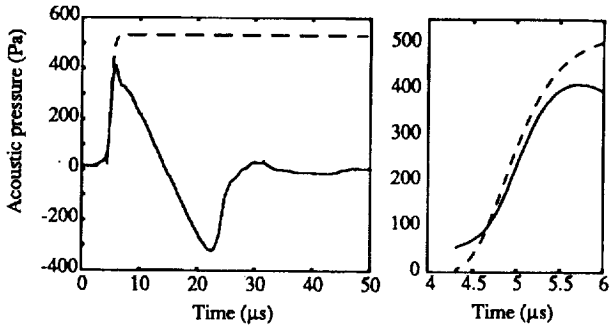

jet nozzle velocity (m/s)	charact. time (μs)	τ_{Pierce} (μs)	$\tau_{meas.}$ (μs)
12.4	0.23	0.554	0.685
18.3	0.32	0.769	0.745
22.7	0.37	0.889	0.922
26.6	0.41	0.984	1.061
31.3	0.46	1.091	1.308

Kulkarny and White (Ref. 5) and White (Ref. 6) developed a model for the plane wave propagation through a 2-D and 3-D, random, isotropic medium. The model is based on geometric acoustics. The results shown here are for a 3-D, random medium. White derived a uniform probability density function $p(t)$ for the occurence of a first caustic. The parameter t is a nondimensional variable. The only information needed about the random medium is its correlation function. Once this information is known, the scaling variable γ is calculated. The graph shows the probability density curve. It is observed that the most likely position for the occurence of a first caustic is at $t = 1.3$. In the table, values for the most likely position of a first caustic and the mean distance to a first caustic are shown. As is noticed, it is possible that an N wave will pass through a caustic. However, it is unlikely that the wave will pass through more than one caustic.

White and Kulkarny: plane wave propagation through a 3-D, isotropic, random medium (geometric acoustics)

- probability density function p(t) for the occurence of a first caustic

$$p(t) = \frac{a_1}{t^4} e^{-a_2 t^{-3}} \qquad t = \gamma^{2/3} s,$$

$$\gamma^2 = 2 \int_0^\infty \left(\frac{1}{r}\frac{\partial}{\partial r}\right)^2 R(r) dr$$

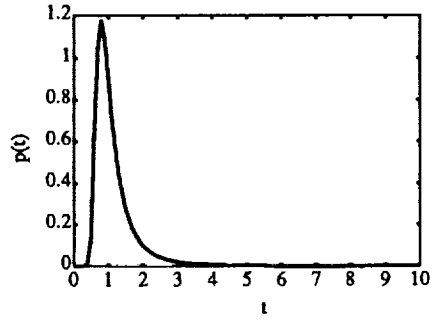

jet nozzle velocity (m/s)	most likely pos. caustic m	mean distance first caustic m
12.4	1.038	1.373
18.3	0.798	1.056
22.7	0.694	0.918
26.6	0.619	0.818
31.3	0.556	0.735

Plotkin and George (Ref. 7) developed a model based on second order scattering theory. They derived a Burgers equation in which the absorption term is a function of the turbulence characteristics. L_0 is the integral length scale, a measure of the eddies of permanent character, and $\epsilon_T = \left\langle \left(\Delta c + \Delta u_{\|}\right)^2 \right\rangle / c_0^2$ is an effective turbulence Mach number. The rise time is determined by the balance between nonlinear steepening and scattering by turbulence. An expression for the rise time is obtained. Plotkin (Ref. 2) compared results from their model with measurements and obtained a good correlation. It is, however, difficult to obtain accurate estimates of the integral length scale and the turbulence Mach number of the atmosphere. A controversy still exists as to whether travel time variations are accounted for correctly or not.

2. Plotkin and George (1972): Second order perturbation theory

$$\frac{\partial P}{\partial t} + \frac{c_0(\gamma+1)}{2\gamma}\frac{P}{p_0}\frac{\partial P}{\partial \xi} = \frac{L_0}{c_0}\left\langle \left(\Delta c + \Delta u_{\|}\right)^2 \right\rangle \frac{\partial^2 P}{\partial \xi^2}$$

$$p = p^N + p_1^S + p_2^S$$

$$P = p - p_1^S$$

$$\tau = \frac{16\gamma}{\gamma+1}\frac{p_0}{\Delta p_0}\frac{\left\langle \left(\Delta c + \Delta u_{\|}\right)^2 \right\rangle L_0}{c_0^3}$$

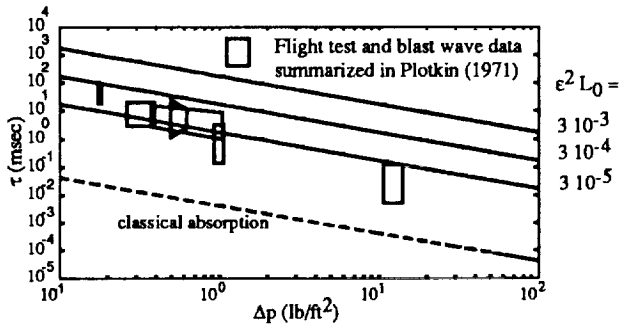

- Problem: travel time variations accounted for?

In order to compare Plotkin's prediction with measurements, we computed the mean waveform in two different ways. First, we computed the mean waveform by shifting the time origins in a similar way as described before and we call this the time shifted mean. Second, we calculated the stochastic mean waveform without any correction for the arrival time of each individual waveform and we call this the stochastic mean. The graph shows an example of the difference for the two computed mean waveforms. As is seen, the stochastic mean presents an insignificant upper bound to the rise time of the time shifted mean.

Again we compare results for five different nozzle velocities. It is noticed that Plotkin and George's prediction has a better correlation with the stochastic mean than with the time shifted mean. A conclusion that seems apparent from the results is that travel time variations of individual waves are not accounted for correctly in Plotkin and George's model.

$$\tau = \frac{16\gamma}{\gamma+1}\frac{p_0}{\Delta p_0}\frac{\left\langle \Delta u_{\parallel}{}^2 \right\rangle L_0}{c_0^3} \qquad \epsilon_t = \frac{\left\langle \Delta u_{\parallel}{}^2 \right\rangle^{1/2}}{c_0}$$

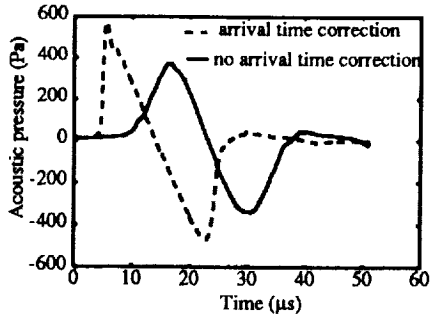

jet nozzle velocity (m/s)	charact. time (μs)	$\tau_{Plotkin}$ (μs)	stoch. mean $\tau_{meas.}$ (μs)	time shifted $\tau_{meas.}$ (μs)
12.4	0.23	1.13	2.767	0.685
18.3	0.32	2.49	3.867	0.745
22.7	0.37	3.78	4.840	0.922
26.6	0.41	5.34	4.833	1.061
31.3	0.46	7.37	5.528	1.308

The last model is that of Ffowcs Williams and Howe (Ref. 8) (FfW & H). In their paper FfW & H mention that the Burgers equation derived by Plotkin and George represents the stochastic mean. FfW & H warn about possible misinterpretation of the results of the Burgers equation as an energy loss, while in reality it describes the loss of coherence of the mean wave because of the random convection of the shock fronts. The model by FfW & H is based on a multiple scattering theory. A diffusion equation is obtained that describes the acoustic energy $\mathcal{E}$ in wavenumber space as a function of the turbulence Mach number m and a length scale Δ related to the Taylor microscale. An expression for the shock thickness δ is derived as a function of the incident shock thickness δ_0 and the integrated scattering diffusivity μ. FfW & H found at most an increase of 30 % in the rise time and concluded in their paper that molecular relaxation must be the cause of the large rise times of booms. Plotkin (Ref. 9) argued that since his model does not yield an acoustic energy loss but just a spatial relocation, one would not expect a change in rise time according to the definition employed by FfW & H.

3. Ffowcs Williams and Howe (1973): Multiple scattering

- Plotkin's approach describes stochastic mean properties of boom

- Multiple scattering theory: diffusion equation for distribution of acoustic energy in wavenumber space

$$\frac{\partial \mathcal{E}(\mathbf{k})}{\partial t} + c_0 \frac{\partial \mathcal{E}(\mathbf{k})}{\partial x_{\parallel}} = \frac{c_0 m^2 k^2}{2\Delta} \nabla_{\perp}^2 \mathcal{E}(\mathbf{k})$$

$$\frac{1}{\Delta} = \frac{\pi}{2u^2} \int_0^{\infty} \kappa E(\kappa) d\kappa$$

$$\delta = \delta_0 \left[1 + \mu(x)\right]$$

$$\mu(x) = 2 \int_0^x \frac{m(\xi)^2}{\Delta(\xi)} d\xi$$

- At most a 30 % increase in rise time

- Molecular relaxation is responsible for large rise time

- Problem: phase scrambling is not accounted for

The upper graph presents a comparison of the energy spectrum of an ideal N wave, its rise time and duration equal that of the spark-produced N wave, with the averaged spectrum of 200 N waves recorded in the absence of turbulence. The energy spectrum of the spark-produced N waves closely resembles that of an ideal N wave. The troughs and peaks of the measured spectrum are more rounded than that of the ideal N wave.

The middle graph shows a comparison of the averaged energy spectrum of 200 N waves recorded in the absence of turbulence with that of 200 N waves measured after propagation through the plane jet turbulence. Again, both spectra are very similar, and troughs and peaks are more rounded for the N waves that propagated through the turbulent medium. However, no significant redistribution of acoustic energy is observed in the spectrum, as was predicted by Ffowcs Williams and Howe.

The table presents a comparison between the prediction of Ffowcs Williams and Howe and the measured values for the rise time. Ffowcs Williams and Howe's model clearly yields values for the rise time that are much smaller than the measured ones.

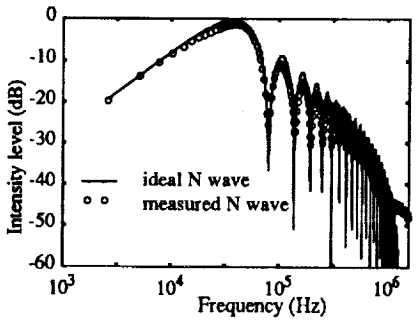

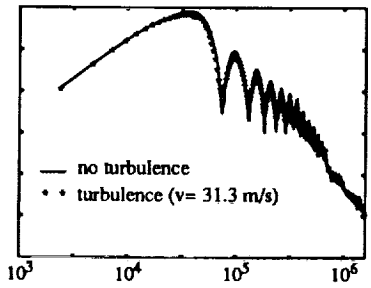

jet nozzle velocity (m/s)	μ	τ_{F-H} (μs)	$\tau_{meas.}$ (μs)
12.4	0.0027	0.687	0.685
18.3	0.0047	0.688	0.745
22.7	0.0067	0.690	0.922
26.6	0.0090	0.691	1.061
31.3	0.0116	0.693	1.308

A new model has been developed for plane wave propagation through a statistically random, isotropic medium (Ref. 3). The random medium consists of a turbulent velocity field. A linear acoustic wave equation (Ref. 2) is derived in which first and second order turbulence effects are included. A perturbation scheme is used to solve the wave equation up to second order.

The turbulent velocity field model was developed by Karweit *et al.* (Ref. 10). Von Kármán's model for incompressible, isotropic turbulence is used to obtain an expression for the 3-D turbulence energy density spectrum. The spectrum is characterized by two length scales. L_0 is an outer length scale, and η is the Kolmogorov microscale.

The 1-D energy spectrum of the plane jet was measured by hot-wire anemometry. If we assume the turbulence is isotropic, the 3-D energy spectrum can be derived. A good agreement is reached between the model and the measurement.

New numerical model for plane wave propagation through a statistically random, isotropic medium

- Turbulent velocity field model
- Linear acoustic wave equation, second order turb. effects
- Perturbation solution
- Results

1. Turbulent velocity field model (Blanc-Benon, Comte-Bellot, 1991)

- Von Kármán's model for incompressible, isotropic turbulence

$$\mathrm{E}(k) = \frac{55}{9}\frac{\Gamma(5/6)}{\sqrt{\pi}\Gamma(1/3)}\frac{u'^2}{L_0^{2/3}}\frac{k^4}{\left(k^2+L_0^{-2}\right)^{17/6}}\exp\left(-2.25(\eta k)^{4/3}\right)$$

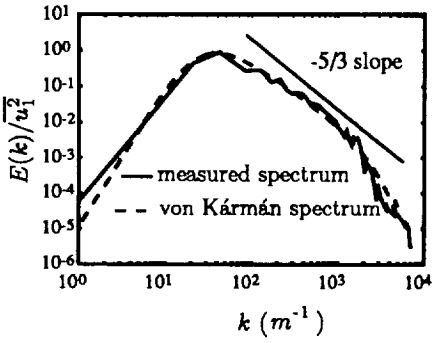

The turbulent velocity field consists of a sum of discrete Fourier velocity modes that are randomly oriented in space. The wave vector geometry of a single Fourier velocity mode is shown in the first graph. The angles θ and ϕ determine the orientation of the wavevector $\mathbf{k}$. The probability density function of both angles are chosen in order to ensure statistical entropy with respect to $\mathbf{k}$. With each turbulence wave vector, a velocity vector $\mathbf{a}(k)$ is associated. Because the turbulent velocity field is incompressible, the velocity vector lies in a plane perpendicular to $\mathbf{k}$. The random angle ψ determines the direction of $\mathbf{a}(k)$. The amplitude of $\mathbf{a}(k)$ is defined by von Kármán's spectrum. A random phase angle γ is attributed to each Fourier mode. A final expression for the turbulent field is obtained as a sum over all the modes.

Wave vector geometry of a single Fourier velocity mode

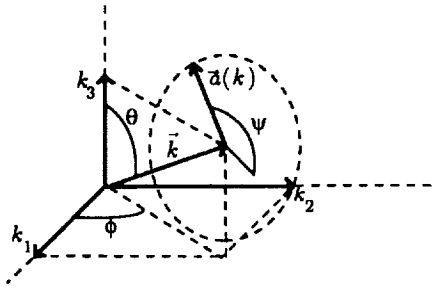

- wavenumber $\mathbf{k}$ is randomly oriented: $P(\theta) = \sin\theta/2$ and $P(\phi) = 1/2\pi$
  statistical isotropy with respect to $\mathbf{k}$

- velocity vector $\mathbf{a}(k)$ -> in plane perpendicular to $\mathbf{k}$
  ψ is random
  $\mathbf{a}(k) \sim \sqrt{\mathbf{E}(k)\Delta k}$
  phase γ of $\mathbf{a}(k)$ is random

- $\mathbf{u}_T(\mathbf{x}) = \sum_{j=1}^{N} |\mathbf{a}_j| \cos(\mathbf{k}_j \cdot \mathbf{x} + \gamma)$

A linear acoustic wave equation is derived. First and second order turbulence effects are retained in the wave equation. We assume that the wave propagation is lossless (isentropic) and that the turbulence is frozen. We only consider velocity fluctuations and do not include thermal fluctuations. ϵ_a is the acoustic Mach number and ϵ_T is the turbulence Mach number.

A regular perturbation scheme in the turbulence Mach number is employed to solve the wave equation. The N wave generated at the focus of the mirror is the boundary condition and it is represented as a sum of its Fourier components.

2. Linear acoustic wave equation

- lossless wave propagation
- the turbulence is frozen
- only turbulent velocity field is present
- wave equation

$$\Box^2 p = -\frac{2}{c_\infty^2}\mathbf{u}_T \cdot \nabla \frac{\partial p}{\partial t} - 2\frac{\partial u_{Tj}}{\partial x_i}\frac{\partial}{\partial x_j}(\int \nabla p dt)_i \qquad \epsilon_a \epsilon_T$$

$$+ 2\frac{\partial u_{Tj}}{\partial x_i}\frac{\partial}{\partial x_j}(\int (\mathbf{u}_T \cdot \nabla) \int \nabla p dt dt)_i \qquad \epsilon_a {\epsilon_T}^2$$

$$+2\frac{\partial U_{Tj}}{\partial x_i}\frac{\partial}{\partial x_j}(\int (\int \nabla p dt \cdot \nabla)\mathbf{u}_T dt)_i - \frac{1}{c_\infty^2}(\mathbf{u}_T \cdot \nabla)(\mathbf{u}_T \cdot \nabla p) \qquad \epsilon_a {\epsilon_T}^2$$

$$+\frac{1}{c_\infty^2} p \nabla \cdot ((\mathbf{u}_T \cdot \nabla)\mathbf{u}_T) \qquad \epsilon_a {\epsilon_T}^2$$

3. Perturbation scheme

$$p = p_0 + \epsilon_T p_1 + {\epsilon_T}^2 p_2 + \ldots$$

$$\text{B.C.} \quad p(0,t) = p_N(t)$$

$$p_N(t) = \sum b_n \sin n\omega_0 t$$

Results from the first order solution are shown here. Each graph represents the sum of the incident N wave and the first order pressure perturbation after propagation through a single realization of the turbulent velocity field. As one observes, the first order pressure perturbation is responsible for the distortion of the N waves. Variations in waveform from peaked to rounded are noticed. Double-peaked and multiple-peaked waveforms are also shown. In some cases (e.g., the rounded waveform), the rise time of the waveform is changed, in other cases it is unaltered. However, the arrival time of each wave is the nominal arrival time (i.e., that of the incident wave). A calculation of the second order pressure perturbation is necessary.

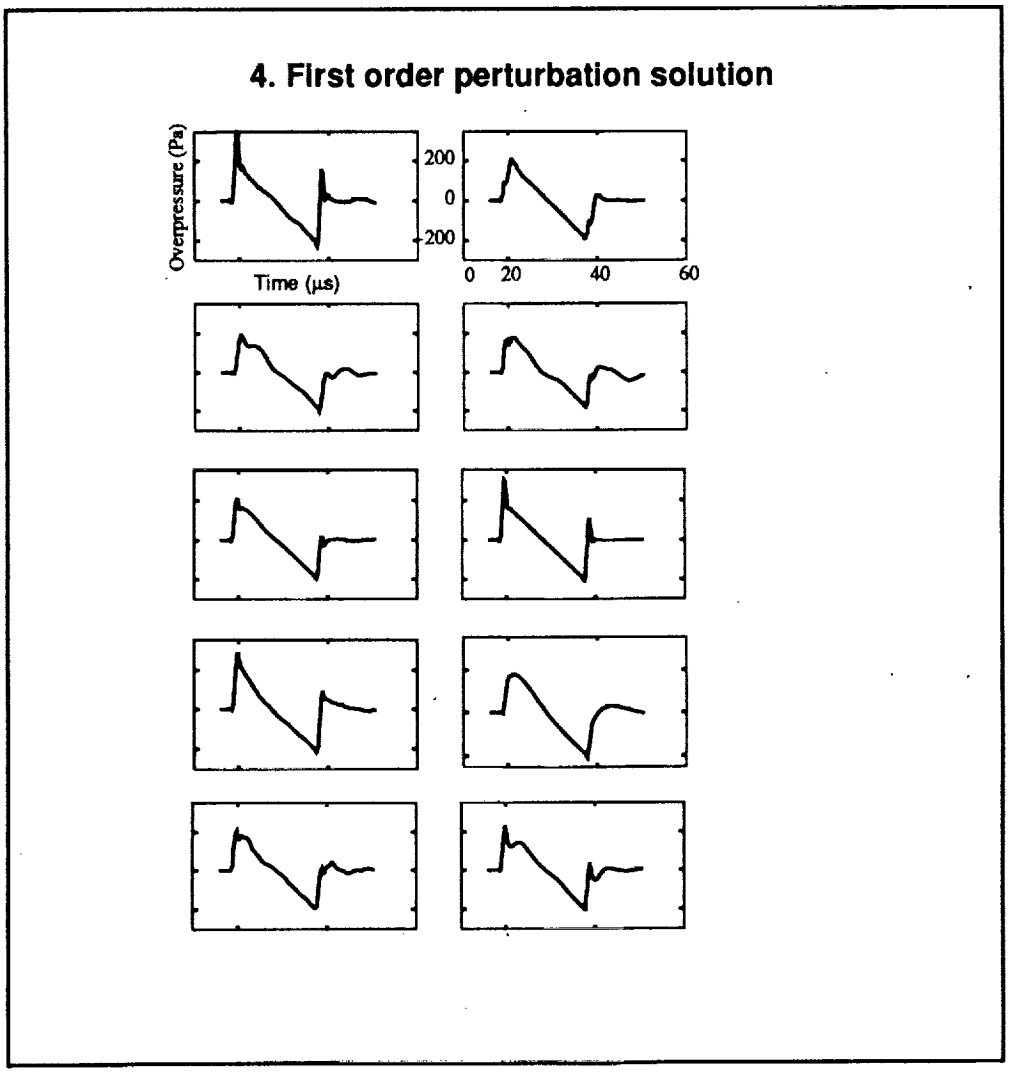

The second order equation that has to be solved contains two secular terms and regular terms. A solution for the second order pressure perturbation is obtained.

The total solution consists of the incident wave, the first order pressure perturbation, and the second order pressure perturbation due to the secular and regular terms. A renormalization technique is used to strain the z-coordinate. The straining of the z-coordinate is used to remove one of the singularities. The final solution is then written as a sum of the Fourier components of the N wave. The second order singularity introduces changes in the phase speed. At second order, the phase speed becomes dependent on the turbulence characteristics.

5. Second order perturbation solution

$$\Box^2 {\epsilon_T}^2 p_2 = (\alpha - \beta - \gamma) \sin n\omega_0\left(t - \tfrac{z}{c_\infty}\right) - \delta \cos n\omega_0\left(t - \tfrac{z}{c_\infty}\right), \quad p_2(0,t) = 0$$

$$+ \text{ regular terms}$$

$${\epsilon_T}^2 p_2 = -\frac{(\alpha - \beta - \gamma)c_\infty}{2n\omega_0} z \cos n\omega_0\left(t - \tfrac{z}{c_\infty}\right) + \frac{\delta c_\infty}{2n\omega_0} z \sin n\omega_0\left(t - \tfrac{z}{c_\infty}\right)$$

$$+ \text{ regular terms}$$

6. Total solution

$$p = b_n \sin n\omega_0\left(t - \tfrac{z}{c_\infty}\right) + \epsilon_T p_1$$

$$-\frac{(\alpha - \beta - \gamma)c_\infty}{2n\omega_0} z \cos n\omega_0\left(t - \tfrac{z}{c_\infty}\right) + \frac{\delta c_\infty}{2n\omega_0} z \sin n\omega_0\left(t - \tfrac{z}{c_\infty}\right)$$

$$+ \text{ regular terms of order } {\epsilon_T}^2 \text{ or higher}$$

Renormalization technique (strained coordinate)

$$z = s(1 + {\epsilon_T}^2 \omega_1 + \ldots)$$

Final solution $$p = \sum_n (1 + {\epsilon_T}^2 \omega_2 z) \sin n\omega_0\left(t - \frac{z}{c_\infty(1 + {\epsilon_T}^2 \omega_1)}\right) + \epsilon_T p_1$$

- $\epsilon_T p_1$ is first order perturbation solution
- ${\epsilon_T}^2 \omega_1 = -\dfrac{(\alpha - \beta - \gamma)}{2b_n\left(\frac{n\omega_0}{c_\infty}\right)^2}$
- ${\epsilon_T}^2 \omega_2 = \frac{\delta c_\infty}{2n\omega_0}$

Results from the numerical simulations that incorporate the second order effects are shown. The phase speed is a function of the turbulence characteristics, and the actual phase speed is different from the nominal phase speed. Small variations in arrival time are observed. It is seen that a combination of first and second order effects of the turbulent velocity field is needed to fully explain the waveform distortion and the change in rise time.

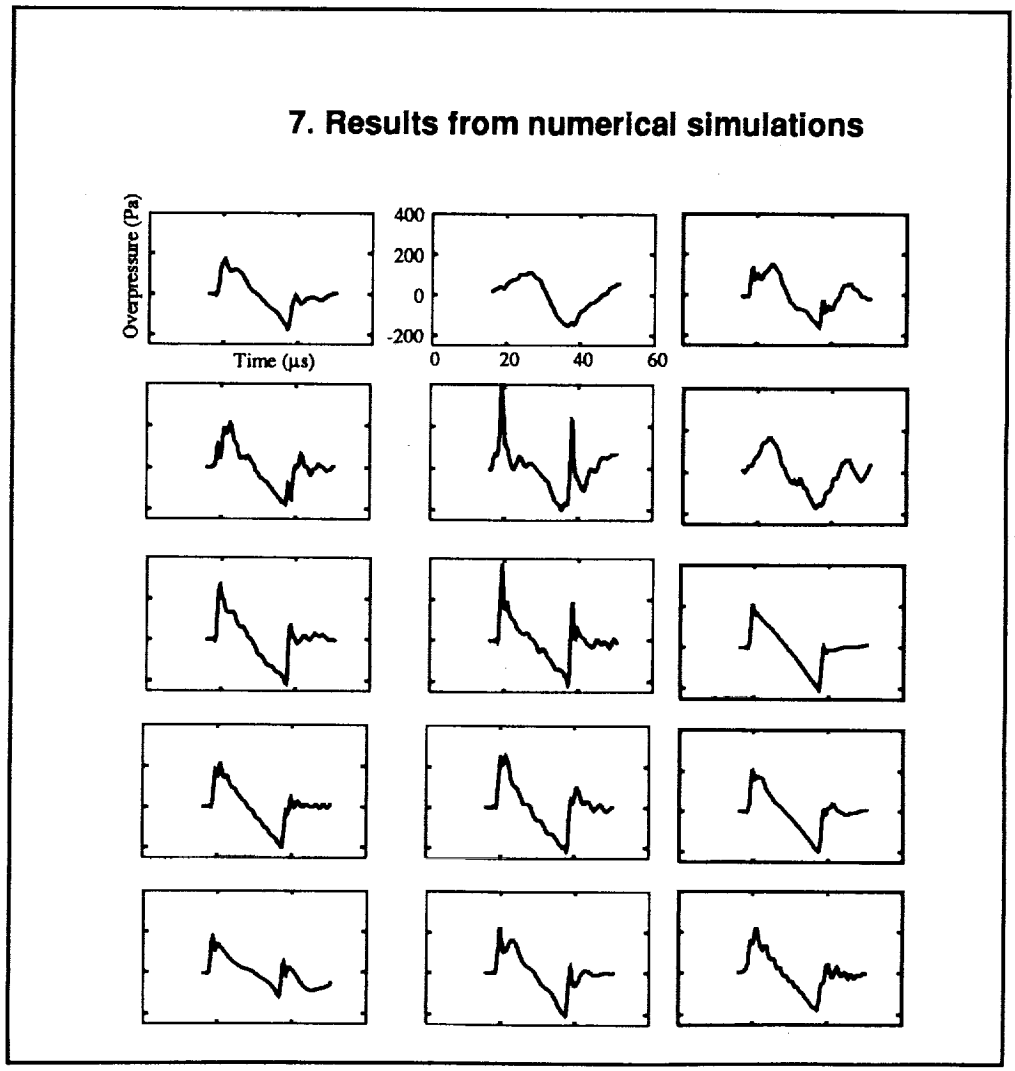

In order to make a convincing statement that the theoretical model is capable of simulating the propagation of plane N waves through a turbulent medium, we compared computed waveforms of the theoretical model with actual measured waveforms of the model experiment. The upper traces represent waveforms computed by the theoretical model, while the lower traces show waveforms from the model experiment.

Two examples are given of a spiked waveform, and two examples of a rounded waveform. As one notices, the waveforms from the theoretical model exhibit the same distortion and change in rise time as that of the model experiment.

8. Comparison of numerical simulations and measured waveforms

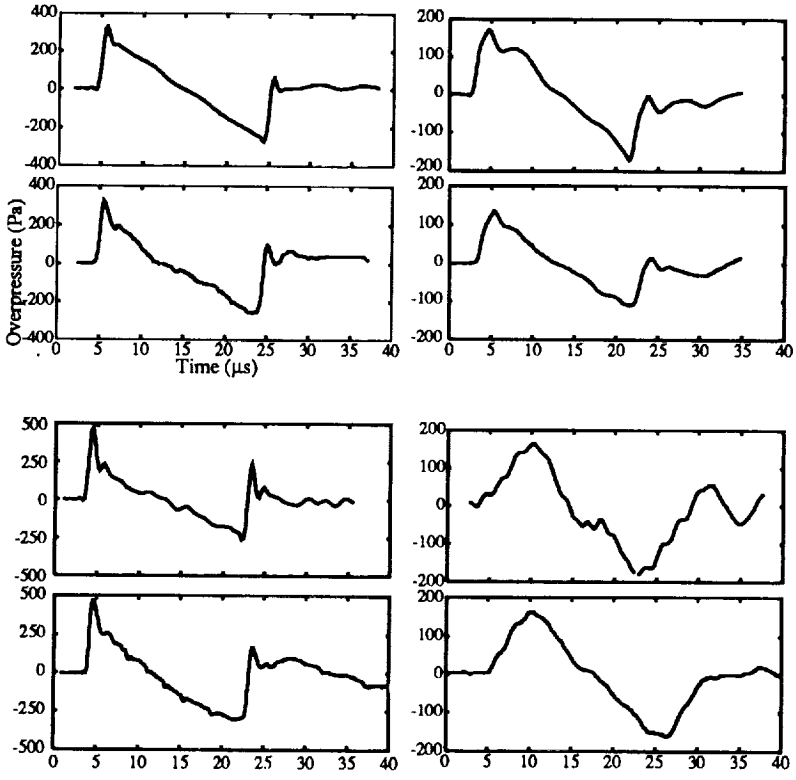

Comparisons of double-peaked waveforms are shown, and also a comparison of a U-shaped waveform and a rounded waveform is presented.

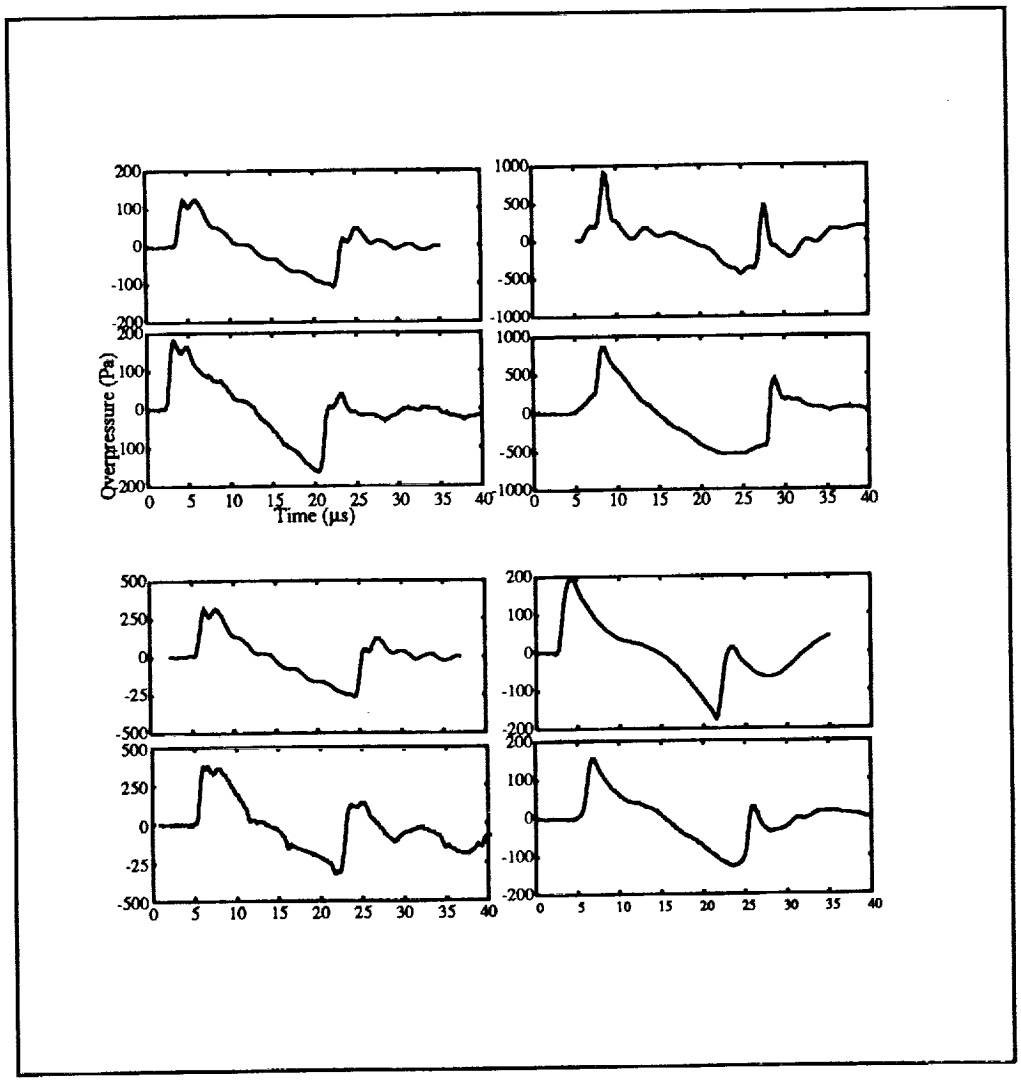

We showed that a model experiment can be successful in simulating the propagation of sonic booms through atmospheric turbulence.

We also reviewed sonic boom models and compared the data from the model experiment with the results from the models. We found that only Pierce's wavefront folding model is fairly accurate and that results from other models are not confirmed by the model experiment data.

A new theoretical model is developed in which plane waves propagate through single realizations of a turbulent velocity field. The wave equation is solved by a perturbation method. The first order pressure perturbation creates the distortion of the N wave, and at second order a singularity occurs. The second order singularity introduces changes in the phase speed. The results from the theoretical model are confirmed by comparison with measured waveforms from the model experiment.

Conclusion

- model experiment is successful

- reviewed sonic boom models
  - only Pierce's model is fairly accurate
  - others are not confirmed by model exp. data

- developed new theoretical model
  - waves are propagated through single realizations of turbulent velocity field
  - second order solution introduces a dispersion effect
  - waveform distortion and change in rise time is caused by dispersion effect
  - results are confirmed by comparison with measured waveforms

Bibliography

1 Crow, S. C. (1969). " Distortion of sonic bangs by atmospheric turbulence," *J. Fluid. Mech.* **37**, 529-563.

2 Plotkin, K. J. (1971). *The effect of atmospheric inhomogeneities on the sonic boom,* Ph. D. Thesis, Cornell University.

3 Lipkens, B. (1993). *Experimental and theoretical study of the propagation of N waves through a turbulent medium,* Ph. D. Thesis, The University of Texas at Austin.

4 Pierce, A. D. (1971). "Statistical theory of atmospheric turbulence effects on sonic boom rise times," *J. Acoust. Soc. Am.* **49**, 906-924.

5 Kulkarny, V. A., and White, B. S. (1982). "Focusing of waves in turbulent inhomogeneous media," *Phys. Fluids* **25**, 1770-1784.

6 White, B. S. (1984). "The stochastic caustic," *SIAM J. Appl. Math.* **44**(1), 127-149.

7 Plotkin, K. J., and George, A. R. (1972). "Propagation of weak shock waves through turbulence," *J. Fluid. Mech.* **54**(3), 449-467.

8 Ffowcs Williams, J. E., and Howe, M. S. (1973). "On the possibility of turbulent thickening of weak shock waves," *J. Fluid. Mech.* **88**, 563-583.

9 Plotkin, K. J. (1989). "Review of sonic boom theory," AIAA 12th Aroacoustics Conference, AIAA-89-1105, April 10-12, San Antonio, TX.

10 Karweit, M., Blanc-Benon, Ph., Juvé, D., and Comte-Bellot, G. (1991). "Simulation of the propagation of an acoustic wave through a turbulent velocity field: a study of phase variance," *J. Acoust. Soc. Am.* **89**(1), 52-62.